JACS
JOURNAL OF THE AMERICAN CHEMICAL SOCIETY

Communication

pubs.acs.org/JACS

Spectroscopic and Crystallographic Characterization of "Alternative Resting" and "Resting Oxidized" Enzyme Forms of Bilirubin Oxidase: Implications for Activity and Electrochemical Behavior of Multicopper Oxidases

Christian H. Kjaergaard,[†] Fabien Durand,[‡,⊥] Federico Tasca,[†] Munzarin F. Qayyum,[†] Brice Kauffmann,[§] Sébastien Gounel,[‡,⊥] Emmanuel Suraniti,[‡,⊥] Keith O. Hodgson,[†,∥] Britt Hedman,[∥] Nicolas Mano,*[,‡,⊥] and Edward I. Solomon*[,†,∥]

[†]Department of Chemistry, Stanford University, Stanford, California 94305, United States

[‡]CNRS, CRPP, UPR 8641, F-33600 Pessac, France

[⊥]Universite de Bordeaux, CRPP, UPR 8641, F-33600 Pessac, France

[§]Institut Européen de Chimie et Biologie, F-33607 Pessac, France

[∥]Stanford Synchroton Radiation Lightsource, SLAC, Stanford University, Stanford, California 94309, United States

Supporting Information

ABSTRACT: While there is broad agreement on the catalytic mechanism of multicopper oxidases (MCOs), the geometric and electronic structures of the resting trinuclear Cu cluster have been variable, and their relevance to catalysis has been debated. Here, we present a spectroscopic characterization, complemented by crystallographic data, of two resting forms occurring in the same enzyme and define their interconversion. The resting oxidized form shows similar features to the resting form in *Rhus vernicifera* and *Trametes versicolor* laccase, characterized by "normal" type 2 Cu electron paramagnetic resonance (EPR) features, 330 nm absorption shoulder, and a short type 3 (T3) Cu−Cu distance, while the alternative resting form shows unusually small $A_{\parallel}$ and high $g_{\parallel}$ EPR features, lack of 330 nm absorption intensity, and a long T3 Cu−Cu distance. These different forms are evaluated with respect to activation for catalysis, and it is shown that the alternative resting form can only be activated by low-potential reduction, in contrast to the resting oxidized form which is activated via type 1 Cu at high potential. This difference in activity is correlated to differences in redox states of the two forms and highlights the requirement for efficient sequential reduction of resting MCOs for their involvement in catalysis.

Multicopper oxidases (MCOs) are a large group of enzymes, including laccase, CueO, Fet3p, and bilirubin oxidase (BOD).[1] These enzymes couple single-electron oxidations of various substrates to the four-electron reduction of dioxygen to water.[2] This reactivity involves a minimum of four Cu ions, arranged in a type 1 (T1) Cu and a trinuclear Cu (TNC) site.[3] The T1 Cu, ranging in potential from +350 to +800 mV,[4] receives electrons from the substrate and transfers them to the TNC, which is the site of dioxygen reduction.[5] A generally accepted reaction mechanism for O_2 reduction by the TNC involves two two-electron transfers, starting from a fully reduced enzyme.[6] In the first step, O_2 is reduced by two electrons, forming the so-called peroxy intermediate (PI). This is followed by a second two-electron transfer, which results in cleavage of the O−O bond and formation of a second intermediate, the native intermediate (NI). The catalytic cycle is completed upon reduction of NI by a total of four electrons, regenerating a fully reduced enzyme.[6]

Different resting forms of MCOs have been observed, and there has been some debate as to which is the relevant form for activation for catalysis.[7] The best-characterized form is the as-isolated resting oxidized form observed in *Rhus vernicifera* and *Trametes versicolor* (TvL). This resting form is also obtained in the decay of NI in the absence of reducing substrate.[8] In the resting oxidized form, the TNC is fully oxidized, with spectroscopically defined mononuclear T2 Cu(II) and binuclear T3 Cu(II) sites. The T2 Cu(II) is magnetically isolated, with "normal" electron paramagnetic resonance (EPR) parameters of $g_{\parallel} = 2.22-2.27$ and $A_{\parallel} = 170-200 \times 10^{-4}$ cm^{-1}, and the absence of intense UV/vis absorption features. The T3 Cu(II)'s are antiferromagnetically coupled, with intense charge-transfer transitions around 330 nm, originating from a bridging hydroxide ligand.[2] Correlated crystal structures show an oxygen bridging atom between the T3 Cu's, which are separated by <4 Å[9] (Table 1). In contrast, an alternative resting form of MCOs has been observed primarily in BODs, including CotA from *Bacillus subtilis*. This alternative resting form is characterized by a TNC with an unusually small $A_{\parallel}$ ($80-100 \times 10^{-4}$cm^{-1}),[10] lack of 330 nm absorption intensity, and T3 Cu−Cu distances of >4.7 Å, with a dioxygen or single oxygen bridging the two T3 Cu's[7,11] (Table 1).

Herein, we define both the "resting oxidized" and the "alternative resting" forms of MCOs in the same BOD enzyme and show that they can interconvert. From a detailed

Received: December 20, 2011
Published: March 13, 2012

   dx.doi.org/10.1021/ja211872j | *J. Am. Chem. Soc.* 2012, 134, 5548−5551

Table 1. Spectroscopic and Structural Properties of Resting Forms of MCOs

	EPR: $A_{\|}$, $g_{\|}$	330 nm abs	T3 Cu−Cu distance (Å)
resting oxidized	170−200 × 10^{-4}cm^{-1}, 2.22−2.27	yes	<4
alternative resting	80−100 × 10^{-4} cm^{-1}, 2.34−2.39	no	>4.7

spectroscopic analysis, we identify a difference in the redox states of the TNC in the two forms and correlate this to differences in activation for catalysis and in geometric structure.

BOD from *Magnaporthe oryzae* was expressed in *Pichia pastoris* and purified to homogeneity.[12] The as-isolated enzyme has an intense blue color (i.e., oxidized T1 Cu) and 3.7−3.9 Cu's/molecule, as determined by the biquinoline method and by atomic absorption spectroscopy for the enzyme solution at neutral pH.[12] Figure 1 shows the EPR spectrum (black) of the

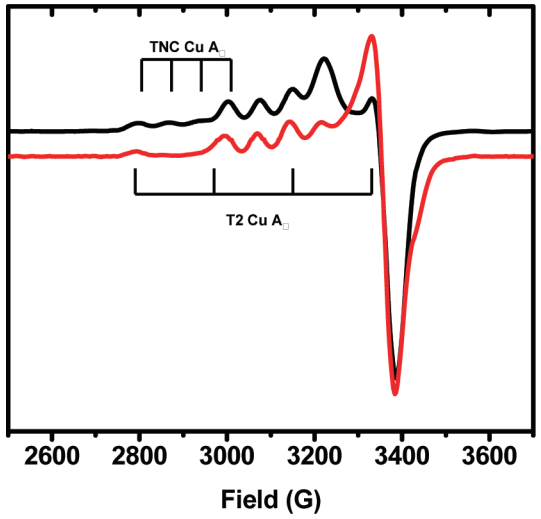

Figure 1. EPR spectra of the as-isolated (black) and reoxidized (red) forms of *M. oryzae* BOD. TNC $A_{\|}$ features are indicated by vertical lines. T1 Cu features are similar in the two forms, with $g_{\|}$ = 2.22 and $A_{\|} \approx 83 \times 10^{-4}$ cm^{-1}.

as-isolated BOD, with spin-integrated intensity of 1.8−1.9 Cu(II)'s per molecule, consistent with one paramagnetic Cu in the TNC (in addition to the oxidized T1 Cu). The EPR parameters of the non-T1 Cu ($g_{\|}$ = 2.37, $A_{\|} = 82 \times 10^{-4}$ cm^{-1}) are similar to those reported for the alternative resting form (Table 1). Interestingly, these features resemble those previously reported for a "type 0" Cu site, observed in mutationally modified T1 Cu from azurin.[13] Furthermore, the absorption spectrum of the as-isolated BOD shows no 330 nm shoulder (Figure S1), again consistent with the alternative resting form (Table 1). To reduce the as-isolated BOD, dithionite was added in small increments to anaerobic enzyme, with concomitant monitoring by EPR. This allowed for selective reduction of the T1 Cu (Figure S2), followed by reduction of the TNC EPR-active Cu. This indicates that the EPR-active TNC Cu has a significantly lower potential than the T1 Cu. Upon complete reduction, the BOD was exposed to dioxygen, which resulted in an immediate return of the blue color, consistent with reoxidation of the enzyme. The TNC EPR features of the reoxidized resting enzyme are considerably different from those of the as-isolated form, as shown in Figure 1 (red), with $g_{\|}$ = 2.24, $A_{\|} = 182 \times 10^{-4}$ cm^{-1}, similar to the resting oxidized form of MCOs (Table 1). Also, the absorption spectrum of the reoxidized enzyme clearly shows the 330 nm shoulder (Figure S1), indicating that all three TNC Cu's have been oxidized. Importantly, when the reoxidized enzyme was exposed to Cl^- ions, a known inhibitor of MCOs, and followed by EPR, regeneration of the alternative enzyme form was observed (Figure S3). It should be mentioned that we observed a similar conversion in commercially available *Myrothecium verrucaria* BOD (Amano 3) from Amano Enzymes Inc. (Figure S4). Based on the above, BOD from *M. oryzae* has two distinct interconvertible resting forms: the resting oxidized form **1**, generated upon reoxidation by O_2 of fully reduced enzyme, and the alternative resting form **2**, observed in the as-isolated enzyme and upon Cl^- addition to **1**.

The electrochemical behaviors of the two resting forms of the BOD in the presence of O_2 were investigated. **1** and **2** respectively were adsorbed on spectrographic graphite electrodes (SPGEs) and subsequently evaluated in air-saturated buffer by cyclic voltammetry. Figure 2 shows the cyclic voltammo-

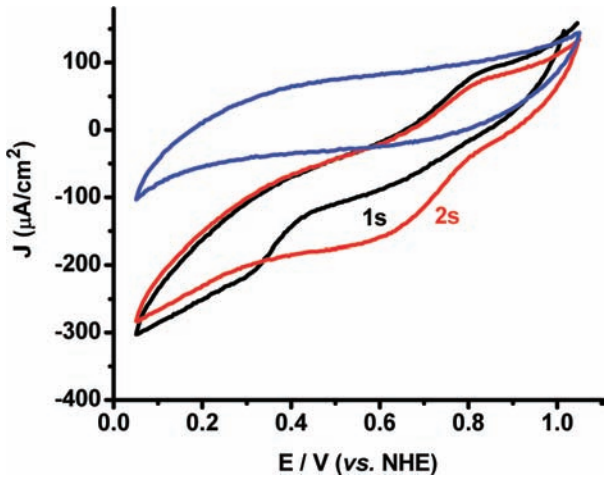

Figure 2. CVs of a polished SPGE (blue), first scan (black, 1 s), and second scan (red, 2 s) of the alternative resting form of *M. oryzae* BOD adsorbed on SPGE in air-saturated sodium phosphate buffer, 0.1 M, pH 6, room temperature. Scan rate 5 mV/s.

grams (CVs) obtained with absorption of the as-isolated alternative form **2**. Compared to the background CV of a bare SPGE electrode (blue), significant catalytic current is observed, verifying activation of the enzyme by direct electron transfer (DET) from the electrode. Importantly, the CVs of the first (black) and second (red) scans are markedly different, with onset of catalytic current observed at ∼+400 mV (vs NHE) in the first scan, shifting to ∼+800 mV in the second scan. A +800 mV onset agrees with previous reports on immobilized BODs, where this was ascribed to DET to the T1 Cu.[14] When the resting oxidized form **1** is adsorbed, catalytic current is also observed (Figure S5). The onset in this case is at ∼+800 mV, thus coinciding with the onset of the catalytic current in the second (and subsequent) scan of **2**. Therefore, the alternative form **2** can be activated for O_2 catalysis only at sufficiently low electrode potentials, consistent with the observation of a low-potential TNC Cu (vide supra), whereas the resting oxidized form **1** is activated at the much higher potential of the T1 Cu. Electrochemical interconversion of **1** and **2**, similar to solution

dx.doi.org/10.1021/ja211872j | *J. Am. Chem. Soc.* 2012, 134, 5548−5551

behavior, was also investigated. Upon electrochemical activation of **2** followed by a resting period of several hours (i.e., no applied potential), the onset current was observed at ~+800 mV (Figure S6). This strongly indicates that, upon reductive activation, the alternative resting form **2** is converted to the resting oxidized form **1**. Also, if an electrode with adsorbed activated enzyme (i.e., resting oxidized form **1**) is placed in NaCl buffer overnight, the CV shows a return to the low activation potential (Figure S7), consistent with the interconversion behavior observed in solution.

Activities of the two resting forms in solution were also explored using 2,2′-azino-bis(3-ethylbenzothiazoline-6-sulfonic acid) (ABTS), a common MCO substrate showing a distinct absorption band upon one-electron oxidation that can be followed spectrophotometrically. Under continuous turnover in air-saturated phosphate buffer, the resting oxidized enzyme showed >10-fold higher activity than the alternative resting form (248 vs 22 units/mg). This is consistent with the high redox potential (+650 mV) of ABTS,[15] again indicating that **2** can only be activated by a sufficiently low reductant (i.e., dithionite), whereas **1** is activated by high-potential substrates. The residual activity of **2** is ascribed to the presence of a small amount of **1**.

To further elucidate differences between the two resting forms of the BOD, we were able to obtain crystals of the as-isolated enzyme, grown for 2 days in pH 4.6 acetate buffer, pH-adjusted with HCl. In order to correlate the crystal structure to the spectroscopy, as-isolated (i.e., alternative resting) enzyme **2** was buffer-exchanged into the crystallization buffer and monitored by EPR over the same time period. After 2 days, this resulted in an EPR spectrum equivalent to that of **2** (Figure S8), verifying that the crystal structure corresponds to the alternative resting form of the enzyme. Under the crystal growth conditions, the resting oxidized form of the BOD, **1**, converts to the alternative resting form, **2**. We are currently pursuing different conditions that may allow crystallization of **1** in BOD. Here, we focus on the structural differences between **1** and **2** of the TNC by comparing the crystal structure of *M. oryzae* BOD (Table S2) **2** to the previously published structure of *T. versicolor* (1GYC)[9b] **1**. The correspondence of the TvL structure to **1** is validated by (a) the equivalent spectroscopic features of the resting oxidized forms in *M. oryzae* BOD (described above) and TvL,[16] (b) the conservation of activity after X-ray exposure of TvL,[9b] and (c) the fact that we found that Cl^- does not convert form **1** to form **2** in TvL.[17] Figure 3 depicts the geometric structures of the TNCs of BOD and TvL, both to resolutions of 1.9 Å. Relevant first- and second-sphere residues are included in addition to the three Cu's. Three oxygen atoms in undefined protonation states are also included. Oxygen (i) is weakly coordinated to the T2 Cu, whereas oxygen (ii) is situated between the two T3 Cu's, in hydrogen-bonding distance (Table S2) to an additional oxygen (iii). It should be mentioned that although the crystallization buffer of the BOD includes chloride ions, no evidence of these was found at or near the TNC (Figure S9). As seen in Figure 3, the overall motif of the TNCs is similar in the two enzyme forms. However, there are two highly important differences. First, the crystal structure of the BOD shows an almost linear T3 Cu–O–Cu angle (171°), in contrast to the 133° angle observed for TvL (Figure 3 and Table S2). Second, the distance between the two T3 Cu's is 5.0 Å in BOD, compared to only 3.9 Å in TvL (Figure 3 and Table S2). A long Cu–Cu distance is in agreement with crystal structures of other BODs, where either

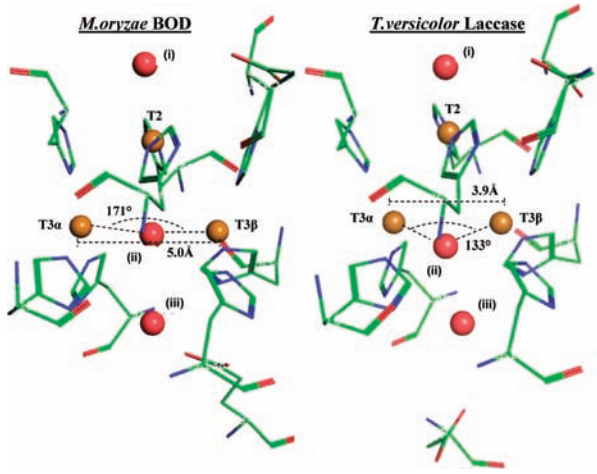

Figure 3. Pymol-generated structures of TNCs in the alternative resting *M. oryzae* BOD and the resting oxidized *T. versicolor* laccase (ATCC 20869, PDB 1GYC). Golden spheres represent Cu atoms, and red spheres represent oxygen. T3 Cu–Cu distances and Cu–O–Cu angles are included.

one or two oxygen atoms are observed in similar positions as oxygen (ii).[7,11]

The origin of the activation, structural, and spectroscopical differences between the two resting forms **1** and **2** was revealed by Cu K-edge X-ray absorption spectroscopy (XAS). Studies on copper-containing model complexes have shown that Cu(I) has an intense transition at 8984 eV, arising from excitation of a core electron from a Cu 1s to its 4p orbitals.[18] This property has been invaluable in determining the redox states of intermediates in MCOs.[19] Figure 4 shows XAS spectra of the

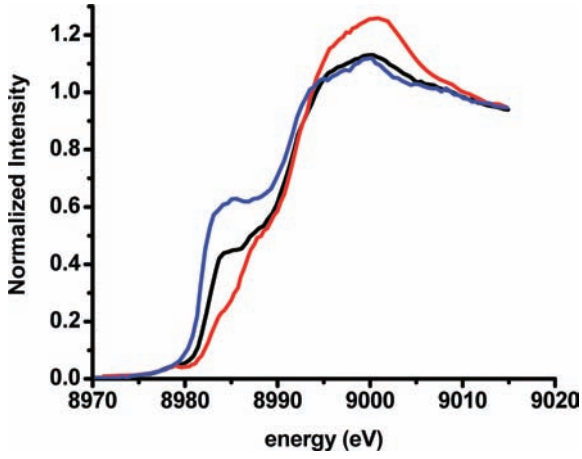

Figure 4. Cu K-edge XAS spectra of as-isolated alternative resting (black), resting oxidized (red), and fully reduced (blue) forms of BOD from *M. oryzae*.

as-isolated alternative form **2** (black) and the resting oxidized form **1** (red) of *M. oryzae* BOD. For comparison, the spectrum of the fully reduced enzyme (blue) is also included. For **1**, very little intensity is observed at 8984 eV, consistent with the spectroscopic features of this site, indicating a fully oxidized enzyme. In contrast, **2** is observed to have significant intensity at 8984 eV, approximately half that observed for the fully reduced enzyme. This, complemented by EPR spin integration and the absence of a 330 nm absorption shoulder, allows assignment of **2** to a 2× Cu(I), 1× Cu(II) TNC (with the T1

dx.doi.org/10.1021/ja211872j | *J. Am. Chem. Soc.* 2012, 134, 5548–5551

Cu oxidized). Importantly, when **2** is regenerated from **1** by the addition of Cl^- ions (vide supra), the XAS edge spectrum is identical to that of as-isolated enzyme **2** (Figure S10), confirming the partially reduced redox state of the alternative resting form **2**. This redox state of **2** may be correlated with the long T3 Cu−Cu distance observed in the crystal structure (vide supra). Structures of MCOs obtained from either crystallography or computations show significantly longer T3 Cu−Cu distances in the fully reduced compared to the fully oxidized forms of the TNC.[20]

In summary, two interconvertible forms of resting MCOs, resting oxidized and alternative resting, have been identified and characterized in the same BOD. The latter is responsible for an unusual TNC EPR signal, a long T3 Cu−Cu distance, and a low redox potential of a TNC Cu. Only the resting oxidized form, **1**, is catalytically active under normal assay conditions, whereas the alternative form, **2**, requires a low-potential reductant to be fully reduced for O_2 reactivity. This reflects the fact that the alternative form has a partially reduced TNC that is not capable of O_2 reduction. This emphasizes the requirement for correct sequential reduction of resting MCO to the fully reduced enzyme, the origin of which is currently being investigated.

■ ASSOCIATED CONTENT

Supporting Information

Experimental procedures, crystal structure coordinates, Figures S1−S10, and Tables S1 and S2. This material is available free of charge via the Internet at http://pubs.acs.org.

■ AUTHOR INFORMATION

Corresponding Author

edward.solomon@stanford.edu

Notes

The authors declare no competing financial interest.

■ ACKNOWLEDGMENTS

This work was supported by a European Young Investigator Award (EURYI), la Région Aquitaine, and by NIH Grants DK-31450 (E.I.S.) and RR-001209 (K.O.H). Portions of this research were carried out at the Stanford Synchrotron Radiation Lightsource, a Directorate of SLAC National Accelerator Laboratory and an Office of Science User Facility operated for the U.S. Department of Energy (DOE) Office of Science by Stanford University. The SSRL Structural Molecular Biology Program is supported by the DOE Office of Biological and Environmental Research, and by the National Institutes of Health, National Center for Research Resources, Biomedical Technology Program. We warmly thank Dr. Pierre Legrand and Andrew Thompson at SOLEIL for beamtime and their help during data collection on PROXIMA1 Beamline. We thank Amano Enzymes inc. for providing Amano 3. F.T. acknowledges the Swedish Chemical Society for financial support (Bengt Lundqvists Post Doc-stipendier 2010). C.H.K. is a Stanford Graduate Fellow.

■ REFERENCES

(1) (a) Reinhammar, B. *Biochim. Biophys. Acta* **1970**, *205*, 35. (b) Outten, F. W.; Huffman, D. L.; Hale, J. A.; O'Halloran, T. V. *J. Biol. Chem.* **2001**, *276*, 30670. (c) Kosman, D. J.; Hassett, R.; Yuan, D. S.; McCracken, J. *J. Am. Chem. Soc.* **1998**, *120*, 4037. (d) Tanaka, N.; Murao, S. *Agric. Biol. Chem.* **1985**, *49*, 1985.

(2) Solomon, E. I.; Sundaram, U. M.; Machonkin, T. E. *Chem. Rev.* **1996**, *96*, 2563.

(3) (a) Allendorf, M. D.; Spira, D. J.; Solomon, E. I. *Proc. Natl. Acad. Sci. U.S.A.* **1985**, *82*, 3063. (b) Spira-Solomon, D. J.; Allendorf, M. D.; Solomon, E. I. *J. Am. Chem. Soc.* **1986**, *108*, 5318.

(4) (a) Kroneck, P. M. H.; Armstrong, F. A.; Merkle, H.; Marchesini, A. In *Ascorbic Acid: Chemistry, Metabolism, and Uses*; Seib, P. A., Tolbert, B. M., Eds.; Advances in Chemistry Series *200*; ACS: Washington, DC, 1982; pp 223−248. (b) Fee, J. A.; Malmstrom, B. G. *Biochim. Biophys. Acta* **1968**, *153*, 299.

(5) Cole, J. L.; Tan, G. O.; Hodgson, K. O.; Solomon, E. I. *J. Am. Chem. Soc.* **1990**, *112*, 2243.

(6) Solomon, E. I.; Augustine, A. J.; Yoon, J. *Dalton Trans.* **2008**, *30*, 3921.

(7) Bento, I.; Silva, C. S.; Chen, Z.; Martins, L. O.; Lindley, P. F.; Soares, C. M. *BMC Struct. Biol.* **2010**, *10*, 28.

(8) Andreasson, L.-E.; Bränden, R.; Reinhammar, B. *Biochim. Biophys. Acta* **1976**, *438*, 370.

(9) (a) Messerschmidt, A; Ladenstein, R.; Huber, R. *J. Mol. Biol.* **1992**, *224*, 179. (b) Piontek, K.; Antorini, M.; Choinowski, T. *J. Biol. Chem.* **2002**, *277*, 37663.

(10) (a) Shimizu, A.; Kwon, J.-H.; Sasaki, T.; Satoh, T.; Sakurai, N.; Sakurai, T.; Yamaguchi, S.; Samejima, T. *Biochemistry* **1999**, *38*, 3034. (b) Martins, L. O.; Soares, C. M.; Pereira, M. M.; Teixeira, M.; Costa, T.; Jones, G. H.; Henriques, A. O. *J. Biol. Chem.* **2002**, *277*, 18849.

(11) Mizutani, K.; Toyada, M.; Sagara, K.; Takahashi, N.; Sato, A.; Kamitaka, Y.; Tsujimura, S.; Nakanishi, Y.; Sugiura, T.; Yamaguchi, S.; Kano, K.; Mikami, B. *Acta Crystallogr.* **2010**, *F66*, 765.

(12) Durand, F.; Gounel, S.; Kjaergaard, C. H.; Solomon, E. I.; Mano, N. *Applied Microb. Biotech.* **2012**, No. DOI: 10.1007/s00253-012-3926-2.

(13) Lancaster, K. M.; George, S. D.; Yokoyama, K.; Richards, J. H.; Gray, H. B. *Nat. Chem.* **2009**, *1*, 711.

(14) (a) Ramirez, P.; Mano, N.; Andreu, R.; Ruzgas, T.; Heller, A.; Gorton, L.; Shleev, S. *Biochim. Biophys. Acta* **2008**, *1777*, 1364. (b) Santos, L.; Climent, V.; Blanford, C. F.; Armstrong, F. A. *Phys. Chem. Chem. Phys.* **2010**, *12*, 13962.

(15) Bourbonnais, R.; Leech, D.; Paice, M. G. *Biochim. Biophys. Acta* **1998**, *1379*, 381.

(16) (a) Malkin, R.; Malmstrom, B. G.; Vanngard, T. *Eur. J. Biochem.* **1969**, *7*, 253. (b) Malkin, R.; Malmstrom, B. G.; Vanngard, T. *Eur. J. Biochem.* **1969**, *10*, 324.

(17) Kjaergaard, C. H.; Solomon, E. I., unpublished results.

(18) Kau, L.-S.; Spira-Solomon, D. J.; Penner-Hahn, J. E.; Hodgson, K. O.; Solomon, E. I. *J. Am. Chem. Soc.* **1987**, *109*, 6433.

(19) (a) Shin, W.; Sundaram, U. M.; Cole, J. L.; Zhang, H. H.; Hedman, B.; Hodgson, K. O.; Solomon, E. I. *J. Am. Chem. Soc.* **1996**, *118*, 3202. (b) Lee, S.-K.; George, S. D.; Antholine, W. E.; Hedman, B.; Hodgson, K. O.; Solomon, E. I. *J. Am. Chem. Soc.* **2002**, *124*, 6180.

(20) (a) Messerschmidt, A.; Luecke, H.; Huber, R. *J. Mol. Biol.* **1993**, *230*, 997. (b) Taylor, A. B.; Stoj, C. S.; Ziegler, L.; Kosman, D. J.; Hart, J. *Proc. Natl. Acad. Sci. U.S.A.* **2005**, *102*, 15459. (c) Yoon, J.; Solomon, E. I. *J. Am. Chem. Soc.* **2007**, *129*, 13127.